Polymerization of Purified Yeast Septins: Evidence That Organized Filament Arrays May Not Be Required for Septin Function

Jennifer A. Frazier,* Mei Lie Wong,* Mark S. Longtine,‡ John R. Pringle,‡ Matthias Mann,§ Timothy J. Mitchison,‖ and Christine Field‖

*Department of Biochemistry and Biophysics, University of California at San Francisco, San Francisco, California 94143; ‡Department of Biology, Univeristy of North Carolina, Chapel Hill, North Carolina 27599; §Protein and Peptide Group, European Molecular Biological Laboratory, D-69012 Heidelberg, Germany; and ‖Department of Cell Biology, Harvard Medical School, Boston, Massachusetts 02115

Abstract. The septins are a family of proteins required for cytokinesis in a number of eukaryotic cell types. In budding yeast, these proteins are thought to be the structural components of a filament system present at the mother–bud neck, called the neck filaments. In this study, we report the isolation of a protein complex containing the yeast septins Cdc3p, Cdc10p, Cdc11p, and Cdc12p that is capable of forming long filaments in vitro. To investigate the relationship between these filaments and the neck filaments, we purified septin complexes from cells deleted for *CDC10* or *CDC11*. These complexes were not capable of the polymerization exhibited by wild-type preparations, and analysis of the neck region by electron microscopy revealed that the *cdc10Δ* and *cdc11Δ* cells did not contain detectable neck filaments. These results strengthen the hypothesis that the septins are the major structural components of the neck filaments. Surprisingly, we found that septin dependent processes like cytokinesis and the localization of Bud4p to the neck still occurred in *cdc10Δ* cells. This suggests that the septins may be able to function in the absence of normal polymerization and the formation of a higher order filament structure.

Key words: cell division • cytokinesis • filaments • *Saccharomyces cerevisiae* • septins

THE septins are a family of proteins originally identified by analysis of budding yeast *cdc* (cell division cycle) mutants defective in cytokinesis (Hartwell, 1971; Cooper and Kiehart, 1996; Longtine et al., 1996). These proteins were initially thought to be unique to yeast, as cytokinesis in yeast and higher eukaryotes appeared to proceed by distinct mechanisms. In recent years, however, septins have also been identified in many other organisms, including humans (Nottenburg et al., 1990; Nakatsura et al., 1994), mice (Kato, 1990; Kumar et al., 1992; Kinoshita et al., 1997; Hsu et al., 1998), and flies (Neufeld and Rubin, 1994; Fares et al., 1995). Almost all of these proteins localize to the future site of division (Neufeld and Rubin, 1994; Fares et al., 1995; Kinoshita et al., 1997; Hsu et al., 1998), and interfering with septin function by mutation or antibody microinjection has been shown to disrupt cytokinesis in budding yeast (Hartwell, 1971), *Drosophila* (Neufeld and Rubin, 1994), and mammalian cells (Kinoshita et al., 1997). In addition to a conserved role in cytokinesis, the septins have also been implicated in a number of processes involving dynamic cell-surface growth and the generation of cell polarity (Chant et al., 1995; Sanders and Herskowitz, 1996; DeMarini et al., 1997; Hsu et al., 1998).

The proteins that comprise the septin family are at least 26% identical in amino acid sequence along their entire lengths. The sequences are not similar to those of any other proteins, except for the presence of a P-loop nucleotide binding motif and other sequences that define the GTPase superfamily (Bourne et al., 1991). Although septins from *Drosophila* have been shown to bind and hydrolyze guanine nucleotide (Field et al., 1996), and mutations in the GTP-binding site alter septin localization in mammalian cells (Kinoshita et al., 1997), the function of nucleotide hydrolysis has not been determined. In addition to the predicted nucleotide binding domain, almost all of the septins are predicted to contain coiled-coil domains at or near their COOH termini. These coiled-coil domains may be involved in interactions between the septins, as recent

Address correspondence to C.M. Field, Department of Cell Biology, 200 Longwood Ave., Harvard Medical School, Boston, MA 02115. Tel.: (617) 432-3727. Fax: (617) 432-3702. E-mail: christine_field@hms.harvard.edu

biochemical studies demonstrate that septins purified from *Drosophila* and mammalian cells form robust complexes (Field et al., 1996; Hsu et al., 1998). These complexes have been shown to form short filaments in vitro, but septin-containing filament structures have not been observed in higher eukaryotic cells by EM.

Evidence that the septins form filaments in cells comes from studies in budding yeast. Studies in wild-type and conditional septin mutants suggest that the septins Cdc3p, Cdc10p, Cdc11p, and Cdc12p are the major structural components of the neck filaments, a series of 10-nm striations that are observed at the future site of cell division by thin-section EM (Byers and Goetsch, 1976). These four septins localize to the region of the neck filaments as assayed by immunofluorescence, and in temperature-sensitive septin mutants, loss of septin localization at the neck correlates with loss of the neck filaments as observed by EM (Byers and Goetsch, 1976; Haarer and Pringle, 1987; Ford and Pringle, 1991; Kim et al., 1991).

The association of the septins with a filament structure that appears to be required for cell division, combined with evidence for nucleotide hydrolysis and filament formation by purified septins, has led to the proposal that the septins comprise a new class of cytoskeletal filaments (Cooper and Kiehart, 1996), similar to intermediate filaments, microtubules, and actin filaments. Polymerization is central to the function of these three well-studied cytoskeletal filaments, whether it be the formation of a rigid structure, the generation of mechanochemical force, or the assembly of a transport track. Thus, mutations or drugs that alter the polymerization behavior of the proteins that make up these filaments radically disrupt the biological processes dependent on them (Amos and Amos, 1991; Alberts et al., 1994; Fuchs and Cleveland, 1998). If the septins are to be thought of as a new class of cytoskeletal filament it must first be determined if, like the filaments described above, septins polymerize in vivo, and if so, to what extent the dynamics and regulation of polymerization are central to septin function. In this study, we use a combination of biochemistry and genetics to investigate the functional relevance of septin polymerization in budding yeast.

Materials and Methods

Strains, Growth Conditions, and Genetic and DNA Methods

The yeast strains used in this study are listed in Table I, with the construction of previously unpublished strains described in detail below. Yeast media (rich solid medium [YPD] and synthetic complete [SC] medium lacking specific nutrients) were prepared as described in Guthrie and Fink (1991). Yeast strains were grown at 22°C unless otherwise noted. Standard methods were used for DNA manipulations and yeast genetics (Sambrook et al., 1989; Guthrie and Fink, 1991) except where noted. PCR reactions were performed using Vent DNA polymerase (New England Biolabs, Beverly, MA) according to the manufacturer's instructions.

Deletion of CDC3, CDC11, and CDC12

The PCR method of Baudin et al. (1993) was used to generate complete deletions of the *CDC3* and *CDC12* coding regions using the *TRP1* plasmid pRS304 as template (Sikorski and Hieter, 1989). Primers for deletion of *CDC3* were cdc3ΔFor 5′-ACGACAACTGAACGATTACATCGGCCTATAATACGTTGCCGATTGTACTGAGAGTGCACC-3′ and cdc3ΔRev 5′-TAATAGTGTATGTTTGAAATTTTTATATGTCTTTATTTCGCTGTGCGGTATTTCACACCG-3′; primers for deletion of *CDC12* were ML58 5′-GAGTATTGATAACGAACTACATCACATATTGTATCAAATAGATTGTACTGAGAGTGCACC-3′ and ML59 5′- AAATTGACGAGACAAAGAGGAAGACATTAATTAATCATCACTGTGCGGTATTTCACACCG-3′. The PCR products were transformed into strain YEF473. Correct integration at the target locus was confirmed by 2+:2− segregation of lethality linked to *TRP1* and by rescue of the lethality by low-copy number plasmids carrying either *CDC3* or *CDC12* (as appropriate) or the appropriate septin gene sequences fused to glutathione-S-transferase (GST)[1] (plasmid: YCp111GST/CDC3 or YCp111GST/CDC12; see below). ML439 and ML437 (Table I) were segregants carrying the GST fusion plamids.

To construct a plasmid for deletion of *CDC11*, a SalI-StuI fragment containing DNA from −1503 to −23 relative to the *CDC11* start codon was ligated into SalI/StuI-digested pJJ248 (Jones and Prakash, 1990) yielding pcdc11Δ5′. Next, a PCR product corresponding to sequences immediately downstream of the *CDC11* stop codon was generated using a *CDC11* plasmid as template and primers 5′-AACAGGATCCCGCTTTTGCCTTCCT-3′ and 5′-AACAGAGCTCGCAGATATAATAAGG-3′. This PCR product was digested with BamHI and SacI at the sites (*underlined*) included in the primers and ligated into BamHI/SacI-digested pcdc11Δ5′, yielding pcdc11Δ::TRP1. That plasmid was then digested with SalI and SacI and used to transform strain YEF473, resulting

1. *Abbreviations used in this paper*: GST, glutathione-S-transferase; HSS, high-speed supernatant.

Table I. Yeast Strains Used in This Study

Strain	Genotype*	Source
YEF473	**a**/a *his3-Δ200/his3-Δ200 leu2-Δ1/leu2-Δ1*	Bi and Pringle, 1996
YEF473A	**a** *his3-Δ200 leu2-Δ1 lys2-801 trp-Δ63 ura3-52*	Bi and Pringle, 1996
YEF473B	α *his3-Δ200 leu2-Δ1 lys2-801 trp-Δ63 ura3-52*	Segregant from YEF473
JAF25	as YEF473 except *cdc10-Δ1/cdc10-Δ1*	This study‡
DDY185-1A	**a** *cdc10-Δ1 his3-Δ200 leu2-Δ1 lys2-801 trp1-Δ63 ura3-52*	DeMarini et al., 1997
ML1366	as YEF473 except *cdc11Δ/cdc11Δ*	See text
ML439	as YEF473B except *cdc3Δ* [YCp111GST/CDC3]	See text
ML424	as YEF473B except *cdc10-Δ1* [YCp111GST/CDC10]	See text
ML426	as YEF473A except *cdc11Δ* [YCp111GST/CDC11]	This study§
ML437	as YEF473A except *cdc12Δ* [YCpGST/CDC12]	See text

**Brackets*, plasmids encoding GST–septin fusions (see text).
‡Constructed by mating appropriate segregants from DDY185 (DeMarini et al., 1997).
§A segregant from DDY185 (DeMarini et al., 1997) transformed with YCp111GST/CDC11.

in deletion of *CDC11* sequences from −23 to the stop codon. Correct integration at the *CDC11* locus was determined by a Southern blot (data not shown). The transformed strain segregated 2+:2− for *TRP1* and the phenotypes of *TRP1* segregants were rescued by a plasmid carrying either *CDC11* or *CDC11* fused to GST sequences (plasmid YCp111GST/CDC11; see below). Strain ML426 was a segregant harboring the latter plasmid. To construct strain ML1366, **a** and α segregants carrying a *URA3 CDC11* plasmid were mated, and the plasmid was cured by growth on plates containing 5-fluoroorotic acid.

Construction of Plasmids Encoding GST–Septin Fusions

Plasmid YCp111GST was constructed by digesting YCplac111 (Gietz and Sugino, 1988) with SmaI and HindIII and ligating to an ~1.8-kb StuI-HindIII fragment from pEGKT (Mitchell et al., 1993) that encodes bacterial GST. Plasmids carrying *CDC3*, *CDC10*, *CDC11*, and *CDC12* fused to GST sequences under the control of the *GAL1/10* promoter were constructed as follows; *underlining* indicates restriction enzyme sites incorporated in the primers to facilitate cloning. The PCR product obtained using a *CDC3* plasmid as template and primers 5′-AATACGGATCCATGAGTTTAAAGGAG-3′ and 5′-CGTTATGTCGACATTATGATATTCTT-3′ was digested with BamHI and SalI and ligated into BamHI/SalI-digested pEGKT. An ~2.5-kb EcoRV-SalI fragment from the resulting plasmid was ligated into SmaI/SalI-digested YCplac111, yielding YCp111GST/CDC3. The PCR product obtained using a *CDC10* plasmid as template and primers 5′-TAATGGATCCCTCAGCTCAGTAC-3′ and 5′-GTACTCTAGAAAA GAAGGTAAAA-3′ was digested with BamHI and XbaI and ligated into BamHI/XbaI-digested pEGKT. An ~2.8-kb SalI-StuI fragment from the resulting plasmid was ligated into SalI/SmaI-digested YCplac111, yielding YCp111GST/CDC10. The PCR product obtained using a *CDC11* plasmid as template and primers 5′-TAACCAAGATCTATGTCCGGAATAATTG-3′ and 5′-TTGCTCGTCGACATTAATACTTTTAAG-3′ was digested with BglII and SalI and ligated into BamHI/SalI-digested YCp111GST, yielding YCp111-GST/CDC11. An XhoI fragment containing *CDC12* from plasmid pEG202/CDC12 (De Virgilio et al., 1996) was ligated into SalI-digested YCp111GST. To place *CDC12* in frame with GST, the resulting plasmid was digested with NcoI, blunt-ended with Klenow enzyme, and then religated. The resulting plasmid was then digested with XbaI, blunt-ended with Klenow enzyme, and then religated, yielding YCp111GST/CDC12. The GST–septin fusion plasmids were all able to complement the appropriate septin deletion strains at 23° and 37°C (data not shown).

Preparation of Anti-Cdc3p Antibodies

The anti-Cdc3p antibody (referred to as PVP antibody) was raised against a synthetic peptide corresponding to the COOH-terminal 15 amino acids of the *Saccharomyces cerevisiae* protein Cdc3p ([C]NHSPVPTKKKGFLR) as described previously (Sawin et al., 1992).

Extract Preparation

Yeast extracts were prepared from log-phase diploid cells based on the method of Kellogg et al. (1995). The extraction buffer used contained 50 mM Hepes, pH 7.6, 75 mM KCl, 0.2% Triton X-100, 1 mM PMSF, 1 mM leupeptin, 1 mM chymostatin, and 1 mM pepstatin. Extraction buffer was mixed with the cell lysate by vortexing and two 10-s pulses of sonication. The yeast high-speed supernatant (HSS) used for purification of the septin complex was obtained by centrifuging this extract at 116,000 *g* for 40 min. In a typical preparation, we used 12 g of frozen yeast cells and obtained 25 ml of yeast HSS with a protein concentration of ~25 mg/ml.

Complex Isolation

The yeast septin complex was purified by modifications of the procedure of Field et al. (1996). Affinity-purified PVP antibody was adsorbed to protein A-Affiprep beads (Bio-Rad Laboratories, Hercules, CA) at room temperature in IP buffer (20 mM Tris-HCl, pH 7.9, 75 mM KCl, 0.5 mM Na_3EDTA, 0.5 mM Na_3EGTA, 8% sucrose). Approximately 500 μg of antibody was used per 500 μl (packed volume) of resin. The remaining procedures were carried out at 4°C. The beads were washed once with 20 vol of 0.1% Tween in TBS and three times with 20 vol of IP buffer. The beads were then added to 25 ml of yeast HSS (see above) and incubated with gentle agitation for 1–3 h. The beads were sedimented, washed once with 20 vol of 0.1% Tween in TBS, and four times with 20 vol of IP buffer. The beads were then poured into a column and drained by gravity. One column volume of elution buffer (20 mM Hepes, pH 7.5, 1 M KCl, 0.5 mM Na_3EDTA, 0.5 mM Na_3EGTA, and 8% sucrose) containing 300 μg/ml PVP peptide was then added. After the column had drained and been stopped, one column volume of elution buffer containing peptide was added to incubate overnight (10–16 h). The column was then allowed to drain by gravity, and eluted with two more column volumes of elution buffer containing peptide. The majority of the yeast septin complex (50 μg) was found in the initial flowthrough and the overnight fraction. The concentrations of septin preparations were estimated by densitometry of SDS-PAGE gels and Bradford assays as described previously (Field et al., 1996).

Protein Identification by Mass Spectrometry

Wild-type septin complexes were subjected to one-dimensional SDS-PAGE, gels were stained with Coomassie brilliant blue R-250, and the four predominant bands were excised. The proteins contained in these gel pieces were identified as described previously in Witke et al. (1998).

Hydrodynamic Analyses

To determine the sedimentation coefficient of the yeast septin complex in 1 M KCl elution buffer, 200 μl of freshly eluted protein at a concentration of ~0.08 μg/μl was loaded onto an 8–40% sucrose gradient and spun for 8 h at 55,000 rpm in a Beckman TLS-55 rotor (Beckman, Palo Alto, CA) at 4°C. The gradient was fractionated and analyzed by SDS-PAGE. The gradients were calibrated on each run with catalase (11.3 S), BSA (4.4 S), and ovalbumin (3.6 S). The Stokes radius was estimated by loading 1 ml of freshly eluted septin complex (~0.07 μg/μl) onto a 24-ml prepacked Superose 6 HR 10/30 column (Pharmacia Fine Chemicals, Piscataway, NJ) that had been equilibrated in elution buffer. This column was calibrated with the standards thyroglobulin (8.5 nm), ferritin (6.1 nm), aldolase (4.81 nm), and ovalbumin (3.05 nm). The native molecular mass of the septin complex was estimated by the method of Siegel and Monty (1966).

Electron Microscopy

Negative stain electron microscopy was performed on purified samples as previously described (Field et al., 1996), except grids were stained with 1% uranyl acetate in 50% methanol. To examine short septin filaments, protein preparations were adsorbed to the grid immediately after peptide elution (see above). To look at the septins in the presence of physiological salt concentrations, septin complexes were dialyzed for 30 min into elution buffer containing 75 mM KCl (instead of 1 M KCl) before being adsorbed to the grid. Thin-section electron microscopy was carried out on samples prepared as described by Byers and Goetsch (1991). Three independent rounds of embedding and sectioning were used to analyze 150 (*cdc10Δ*, *cdc11Δ*) or 200 (wild-type) bud necks for the presence of filament structures. Thin sections were spaced such that the same bud necks were not analyzed more than once for the presence of neck filament-associated structures.

Filament Measurement

To determine the lengths of septin filaments, EM negatives were digitized using UMAX MagicScan software (UMAX Data Systems Inc., Fremont, CA) and measured using NIH Image (Bethesda, MD). Straight filaments from six independent high-salt preparations were measured for each septin complex (wild-type, *cdc10Δ*, or *cdc11Δ*). The frequency of filaments over 70 nm in wild-type high-salt preparations is underrepresented, as most of these filaments were curved. The same method was used to calculate the distance between the long filament pairs observed after septin preparations were dialyzed into 75 mM KCl elution buffer.

Fluorescence Staining of Yeast Cells

Immunofluorescence staining of yeast cells was performed by modifications of the protocol of Pringle et al. (1991). Log-phase cells were fixed with 0.025% glutaraldehyde for 3 min, rinsed with PBS, and then fixed with 3.5% formaldehyde in PBS for 30 min. After fixation, 2×10^8 cells were washed with phosphate buffer and then spheroplasted. Spheroplasted cells were applied to polylysine-coated coverslips and submerged in −20°C MeOH for 6 min and −20°C acetone for 30 s (Novick and Bot-

stein, 1985; Sanders and Herskowitz, 1996). The PVP antibody was used at a concentration of 0.01 mg/ml, and the Bud4 antibody was used at a 1:5 dilution as described in Sanders and Herskowitz (1996). To determine the budding pattern of haploid cells, **a** *cdc10Δ* or **a** wild-type cells (see Table I) were grown to early log phase at 22°C and stained with Calcofluor. More than 200 Calcofluor-stained cells with three or more bud scars were examined for each strain. Cells with single chains of bud scars were scored as budding axially. Photomicrographs were taken on a Nikon Optiphot-2 with a 60× objective (Planfluor 1.40 NA) and a cooled CCD camera (Princeton Scientific Instruments Inc., Monmouth Junction, NJ). Images were transferred to Adobe Photoshop for montaging and printing (Adobe Systems, San Jose, CA).

Results

Isolation of a Septin Protein Complex

To characterize the septins from *S. cerevisiae* biochemically, we purified a septin complex using an immunoaffinity approach based on that of Zheng et al. (1996). The antibody used for immunoisolation was raised to the 14 COOH-terminal amino acids of the yeast septin Cdc3p. This antibody, referred to as PVP, recognized a protein of 70 kD in HSS on Western blots (Fig. 1 *A*, *PVP-WT*). This polypeptide was identified as Cdc3p by showing that the 70-kD band shifted to 95 kD in HSS made from cells carrying a *GST-CDC3* fusion (Fig. 1 *A*, *PVP-GST3*). After protein A beads precoated with PVP antibody were incubated in yeast HSS (Fig. 1 *A*, *HSS*), washed, and incubated in PVP peptide and 1 M KCl, predominantly four polypeptides were eluted (Fig. 1 *A*, *SEP*). Of the four eluted polypeptides, migrating with apparent molecular weights of 70, 62, 50, and 37 kD, only the 70-kD band was recognized by the PVP antibody (data not shown), suggesting that these proteins form a complex. Using mass spectrometry, it was determined that the proteins associated with Cdc3p are the yeast septins Cdc10p, Cdc11p, and Cdc12p. This result was confirmed by isolating the complex from strains expressing NH_2-terminal GST fusions of Cdc10p, Cdc11p, or Cdc12p. In each strain an intact complex was still formed, with the appropriate septin shifted to a higher molecular weight (Fig. 1 *B*). The four septins in this complex and a previously uncharacterized septin, Sep7p, have recently been shown to bind to the protein kinase Gin4p (Carroll et al., 1998). Although we saw a band in some of our preparations that may correspond to Sep7p, in no case was this protein present at more than 15% of the level of Cdc3p. Thus, Cdc3p, Cdc10p, Cdc11p, and Cdc12p are the major components of the complex purified with the PVP antibody.

To examine the strength of the interactions between the septin proteins, the complex was analyzed by sucrose gradient sedimentation (Fig. 1 *C*, *top*) and gel filtration chromatography (Fig. 1 *C*, *bottom*). Cdc3p, Cdc10p, Cdc11p, and Cdc12p cofractionated by both techniques in the presence of 1 M KCl, indicating that they form a stable complex. The native molecular weight of this complex was estimated to be 370 ± 60 kD using the Stoke's radius (10.1 nm) and sedimentation coefficient (9 S) (Siegel and Monty, 1966). By gel densitometry of Coomassie dye binding normalized to the predicted molecular weights, it was estimated that Cdc3p, Cdc10p, and Cdc12p are present in roughly equal stoichiometry, while Cdc11p is substoichiometric. A complex composition of 2 Cdc3p:1 Cdc11p:2 Cdc12p:2 Cdc10p is consistent with stoichiometry estimates calculated using the native molecular weight of the complex and the predicted molecular weights of the four septin polypeptides. However, because native molec-

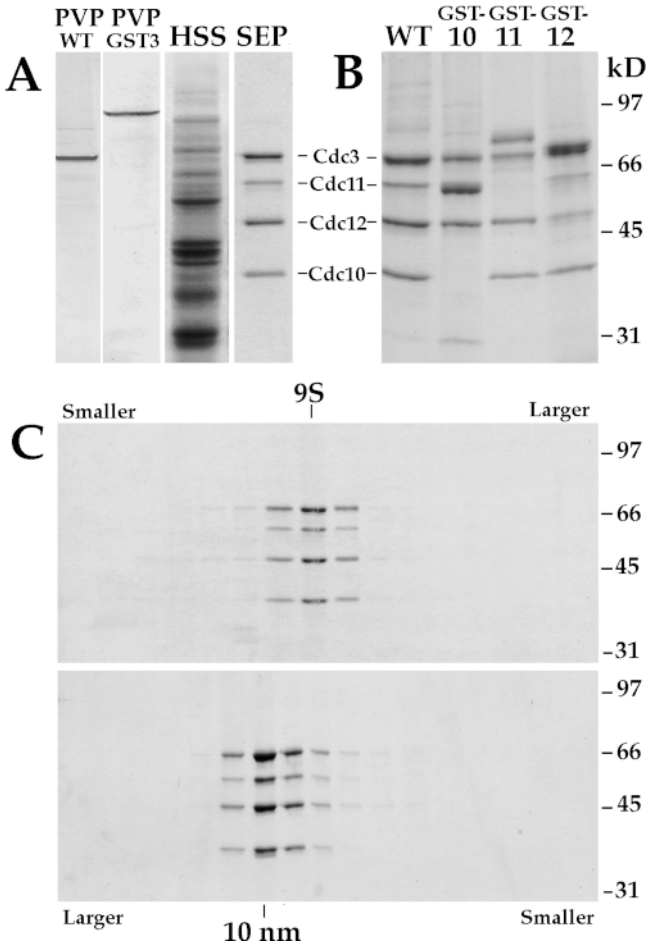

Figure 1. Biochemical characterization of the septin complex. (*A*) *PVP-WT* and *PVP-GST3*, Western blot analyses of HSS made from wild-type cells (*PVP-WT*) or cells in which the endogenous *CDC3* had been replaced with a *GST-CDC3* fusion (*PVP-GST3*), probed with the PVP antibody. *HSS*, Coomassie stain of wild-type yeast HSS. *SEP*, Coomassie stain of polypeptides eluted from the antibody/protein A beads with PVP peptide in the presence of 1 M KCl (septin preparation). (*B*) Complexes purified by PVP antibody affinity from wild-type (*WT*) cells or cells in which the endogenous septin had been replaced with a *GST-CDC10*, *GST-CDC11*, or *GST-CDC12* fusion. Cells were grown in SC-Leucine medium with galactose as a carbon source. Although the majority of Cdc12p changed mobility in the *GST-CDC12* strain, some protein was still apparent at the normal Cdc12p mobility. This is most likely a breakdown product of the GST-Cdc12p fusion and not a distinct protein, as mass spectrometry (see Results) did not reveal another protein in the preparation at this molecular weight. (*C*) Hydrodynamic analyses of the septin preparation in the presence of 1 M KCl elution buffer. The upper gel shows analysis by sedimentation in an 8–40% sucrose gradient. The four identified septin polypeptides cosedimented at 9 S. The lower gel shows analysis by gel filtration chromatography. Fractions from both experiments were analyzed by SDS-PAGE and Coomassie blue staining.

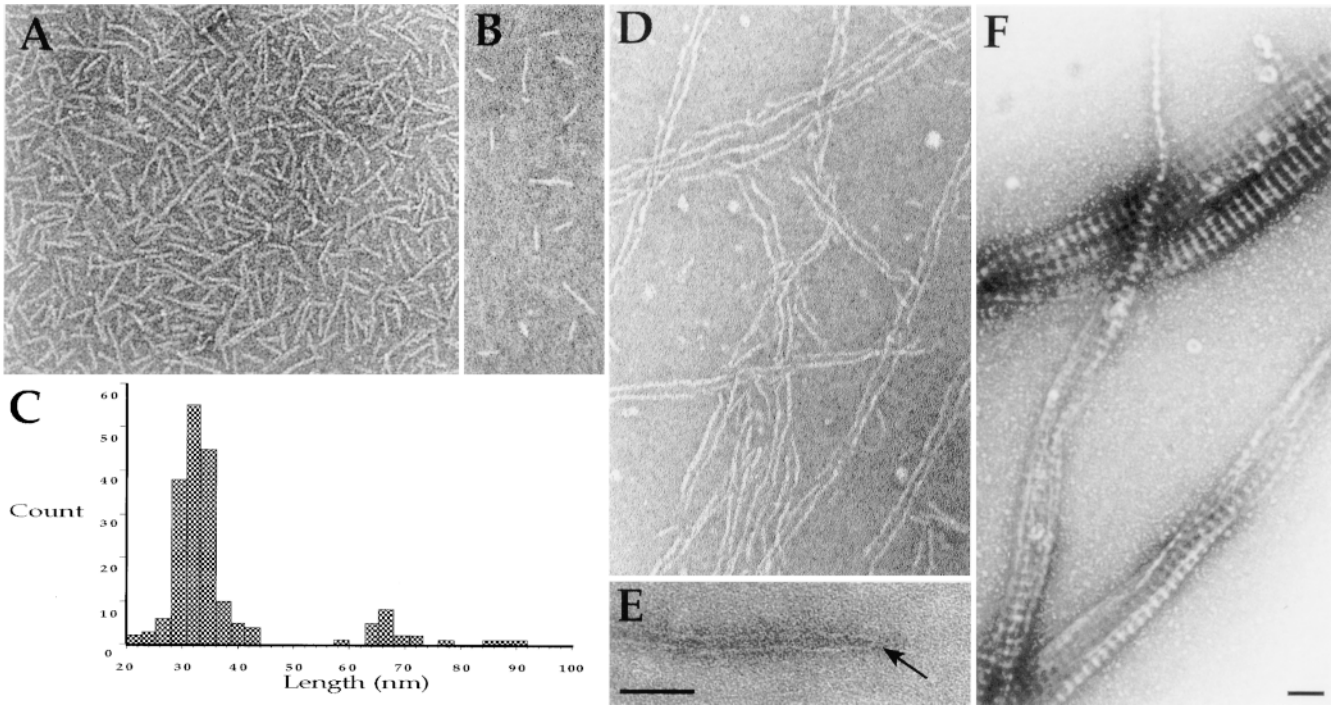

Figure 2. Negative-stain EM of septin filaments. (*A*) Typical wild-type septin preparation adsorbed to the grid after peptide elution in the presence of 1 M KCl. (*B*) A preparation diluted 50-fold in 1 M KCl elution buffer before adsorption to the grid. Samples were diluted to facilitate filament measurement. (*C*) Histogram of the length measurements of septin filaments observed in preparations like that shown in *A* and *B*. (*D*) Long pairs of filaments typically observed after dialysis of a preparation like that seen in *A*, into 75 mM KCl elution buffer. (*E*) An example of the hairpin structures (*arrow*) observed on the ends of some filament pairs in low-salt preparations. (*F*) Paracrystalline arrays of laterally aligned filaments formed by GST-Cdc11p septin complexes after dialysis in 75 mM KCl elution buffer. Bar, 100 nm.

ular weight estimates have at least a 20% margin of error, and Coomassie dye binding is dependent on amino acid composition, alternative stoichiometries or the presence of multiple heterogeneous septin complexes with similar hydrodynamic properties cannot be ruled out.

The Wild-type Septin Complex Forms Long, Paired Filaments

We visualized yeast septin complexes by negative-stain EM to determine if, like septins purified from other organisms (Field et al., 1996; Hsu et al., 1998), these proteins form filaments. In samples eluted from the PVP antibody column in the presence of 1 M KCl, filaments measuring 7–9 nm in diameter and 32–100 nm in length were consistently observed (Fig. 2, *A* and *B*). Length measurements of these filaments revealed a distribution with a periodicity of 32 nm (Fig. 2 *C*), suggesting that the filaments are assembled by the longitudinal association of 32-nm septin subunits.

To observe the septin complex under more physiological conditions, the septin preparation was dialyzed into a buffer containing 75 mM KCl. Under these conditions, filaments ≥1,500 nm in length were observed (Fig. 2 *D*). These filaments were consistently found to form pairs, with the space between filaments ranging from 2–20 nm. Under these conditions, we also observed assemblies containing up to eight aligned filaments (Fig. 2 *D*, *bottom*), and hairpin structures at the ends of some filament pairs (Fig. 2 *E*). The lateral association of septin filaments was especially striking in preparations from a strain in which the endogenous Cdc11p was replaced by an NH_2-terminal GST-Cdc11p fusion (Fig. 2 *F*). These arrays contained over 200 laterally associated filaments and had a striking periodicity of 30 nm.

Septin Complexes Purified from cdc10Δ or cdc11Δ Cells Do Not Form Long Filaments

To begin investigating the functional relevance of these septin polymers in vivo, the effect of deleting individual septin polypeptides on complex assembly and filament formation was studied. Because *cdc3Δ* and *cdc12Δ* cells are inviable, this study was limited to strains deleted for *CDC10* or *CDC11* (Flescher et al., 1993; Longtine et al., 1996). At 22°C, cells deleted for *CDC10* had a shorter doubling time than wild-type cells (Fig. 3 *B*). We found *cdc10Δ* cells grown at this temperature were ovoid, had enlarged bud necks, and sometimes formed clusters of connected cells (Fig. 3 *A*, *cdc10Δ*, 22°C) as previously described (Flescher et al., 1993; DeMarini et al., 1997). After digestion of the cell wall with zymolyase, the relative number of *cdc10Δ* cells doubled (Fig. 3 *B*) and chains of connected cells were no longer observed, indicating that at 22°C these cells are capable of completing cytokinesis by the criteria previously described (Hartwell, 1971). *cdc10Δ*

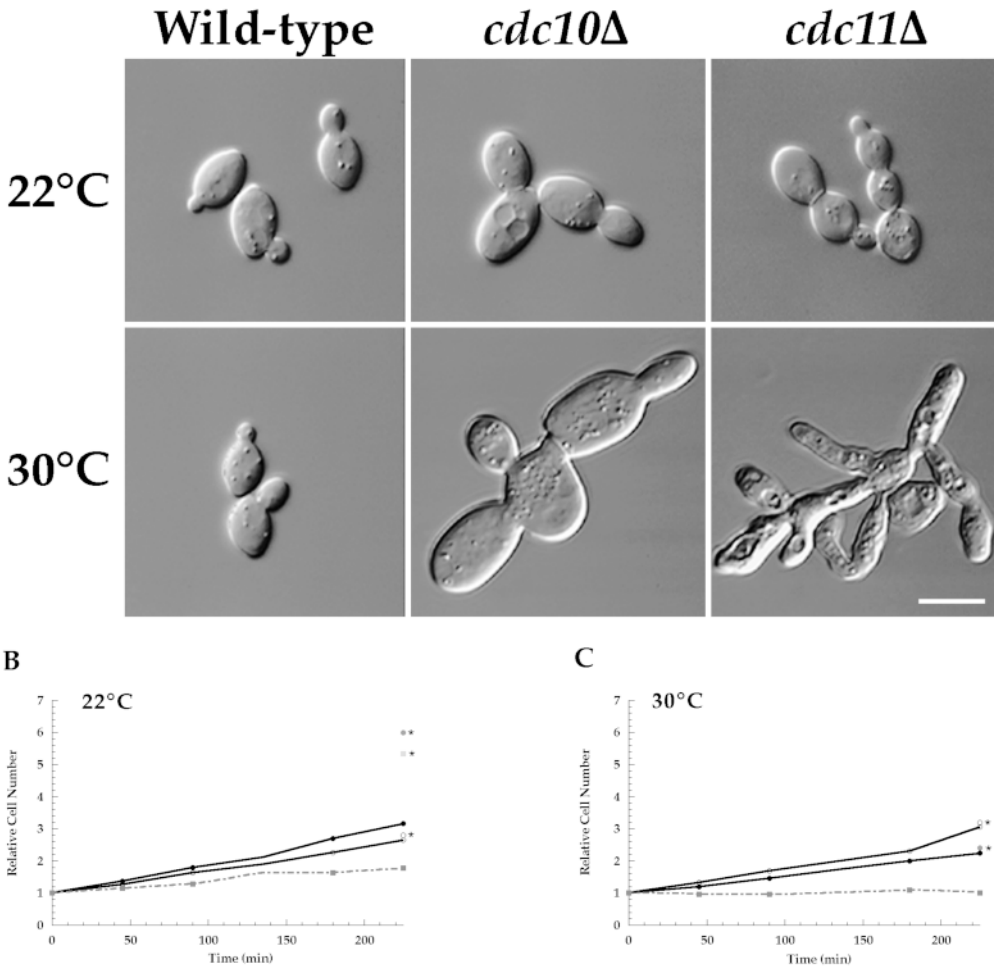

Figure 3. Characterization of septin deletion strains. (*A*) Differential-interference contrast (DIC) micrographs of wild-type, *cdc10Δ*, and *cdc11Δ* diploid cells grown at 22°C or 30°C in YPD to early log phase. (*B* and *C*) Samples were taken at 0, 45, 90, 135, 180, and 225 min from early log-phase cultures grown in YPD at 22°C (*B*) or 30°C (*C*) to examine the growth rates of wild-type, *cdc10Δ*, and *cdc11Δ* cells. Samples from each time point were sonicated and counted on a hemocytometer. The resultant cell concentration at each time point was divided by that at time 0 to give relative cell number, and plotted versus time; *open circles*, wild-type; *closed circles*, *cdc10Δ*; *closed squares*, *cdc11Δ*. *Asterisks*, relative cell number in the 225-min sample after treatment with zymolyase, as described in Lippincott and Li (1998). Over 1,000 cells were counted from each sample in three separate experiments. Bar, 10 μm.

cells did begin to exhibit a cytokinesis defect at higher temperatures. At 30°C, the doubling time of *cdc10Δ* cells increased significantly (Fig. 3 *C*), and connected cells observed at this temperature (Fig. 3 *A*, *cdc10Δ*, 30°C) did not fall apart after cell wall digestion (Fig. 3 *C*). The *cdc10Δ* strain was not viable at temperatures above 30°C (data not shown). We found deleting *CDC11* had a much more severe effect on cell growth and cytokinesis. At 22°C, the *cdc11Δ* strain grew at about half the rate of wild-type cells (Fig. 3 *B*). Cells deleted for *CDC11* formed large clusters of interconnected, elongated cells (Fig. 3 *A*, *cdc11Δ*, 22°C). Although the cell count increased after digestion of the cell wall (Fig. 3 *B*), most cells were still in elongated chains, with up to eight nuclei sharing the same cytoplasm as assayed by light microscopy and thin section EM (see below). *cdc11Δ* cells were not viable at temperatures higher than 22°C (Fig. 3, *A*, *cdc11Δ*, 30°C and *C*). At these elevated temperatures *cdc11Δ* showed no growth and appeared as phase dark branches of cells by light microscopy.

PVP immunoaffinity chromatography was used to purify septin complexes from extracts of *cdc10Δ* or *cdc11Δ* cells grown at 22°C. From the *cdc10Δ* HSS, a complex containing Cdc3p, Cdc11p, and Cdc12p was isolated (Fig. 4 *A*). As in the wild-type complex, Cdc3p and Cdc12p were estimated to be stoichiometric by densitometry of Coomassie-stained gels, whereas Cdc11p appeared to be substoichiometric. When this preparation was visualized by negative-stain EM, only a few small rods of ~24 nm in length could be visualized (Fig. 4, *B* and *C*). Most of the preparation lacked the detectable filament structures seen in wild-type samples. From the *cdc11Δ* HSS, a complex containing the remaining septins (Cdc3p, Cdc10p, and Cdc12p) in approximately equal stoichiometry was purified (Fig. 4 *D*). In these preparations robust short filaments similar to those seen in wild-type preparations were observed (Fig. 4 *E*). Measurement of these short *cdc11Δ* filaments revealed that while most were ~32 nm in length, a large number were either 18 or 22 nm in length (Fig. 4 *F*). These results suggest that complexes containing the remaining septins can form in the absence of Cdc10p or Cdc11p.

Although *cdc10Δ* and *cdc11Δ* septin complexes appear to form short filaments (≤32 nm) in a high-salt buffer, the 64- and 90–100-nm polymers formed by the wild-type septin complex under similar conditions were not observed. This suggested that septin complexes lacking Cdc10p or

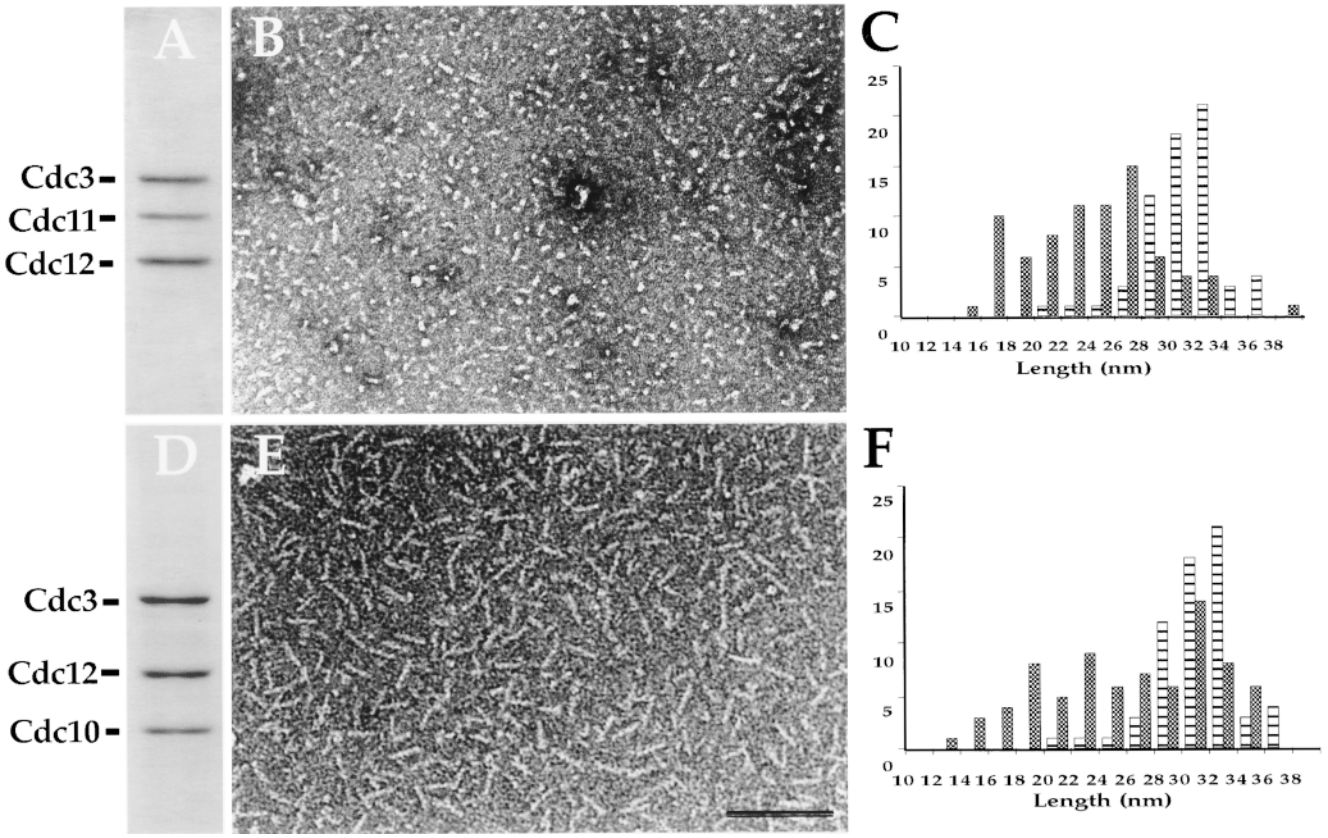

Figure 4. Characterization of septin complexes purified from *cdc10Δ* or *cdc11Δ* cells by PVP affinity chromatography in the presence of 1 M KCl. (*A*) The complex from *cdc10Δ* cells as analyzed by SDS-PAGE and Coomassie blue staining. (*B*) The same preparation visualized by negative-stain EM. (*C*) Histogram of length measurements from the sample shown in *B*. (*D*) SDS-PAGE analysis of the complex from *cdc11Δ* cells. (*E*) The cdc11Δ preparation as visualized by negative-stain EM. (*F*) Histogram of length measurements from the sample shown in *E*. Measurements of wild-type septin filaments (see Fig. 2) are plotted on histograms (*striped columns*) for comparison of septin deletion complexes (*solid columns*). Bar, 100 nm.

Cdc11p might not be capable of the extensive polymerization exhibited by wild-type septin complexes. This hypothesis was tested by dialyzing septin complexes from wild-type, *cdc10Δ*, and *cdc11Δ* cells into low-salt buffer and assaying the formation of long polymers by negative-stain EM and sedimentation. As described above, under these conditions, the wild-type septin preparation formed extremely long polymers and higher order structures (Fig. 5, *Wild-type*, *Low Salt* EM). Furthermore, ~45% of the complex was sedimentable after dialysis into the low-salt buffer (Fig. 5, *Wild-type*, *High* and *Low Salt* gels*)*. Polymerization by *cdc10Δ* or *cdc11Δ* septin complexes could not be detected using either negative-stain EM or the more quantitative sedimentation assay (Fig. 5, *cdc10Δ* and *cdc11Δ*, *High* and *Low Salt* EM and gels). These results suggest that *cdc10Δ* and *cdc11Δ* septin complexes are drastically perturbed in their polymerization behavior compared with the wild-type septin complex.

Neck Filaments Are Not Observed in cdc10Δ or cdc11Δ Cells

To compare in vitro polymerization data with observations of filament structure in vivo, we used thin-section EM to visualize the neck filaments in wild-type, *cdc10Δ*, and *cdc11Δ* cells. The neck filaments were originally described by Byers and Goetsch (1976) as a series of 10-nm striations on the inner surface of the plasma membrane, observable from bud emergence until just before cytokinesis. Using similar procedures, we observed ordered linear structures similar to the previously described neck filaments in 67% of bud necks in asynchronous wild-type cells (Fig. 6, *A′–D′*) (Table II). Such ordered linear structures were not observed in the bud necks of *cdc11Δ* cells (Fig. 6, *A* and *B*) (Table II) or in the vast majority of *cdc10Δ* cells (Fig. 6 *C*) (Table II). Among 150 *cdc10Δ* bud necks examined by thin-section EM, only one appeared to have what might have been neck filaments in cross section (Fig. 6 *D*) (Table II).

Localization of Cdc3p and Bud4p in Wild-type, cdc10Δ, and cdc11Δ Cells

By immunofluorescence, the septins localize to a ring in the region where the neck filaments are visualized by EM, and loss of neck filaments correlates with a loss of septin localization in conditional septin mutants at the nonpermissive temperature (Haarer and Pringle, 1987; Ford and Pringle, 1991; Kim et al., 1991). To examine septin localization in cells with and without observable neck filament

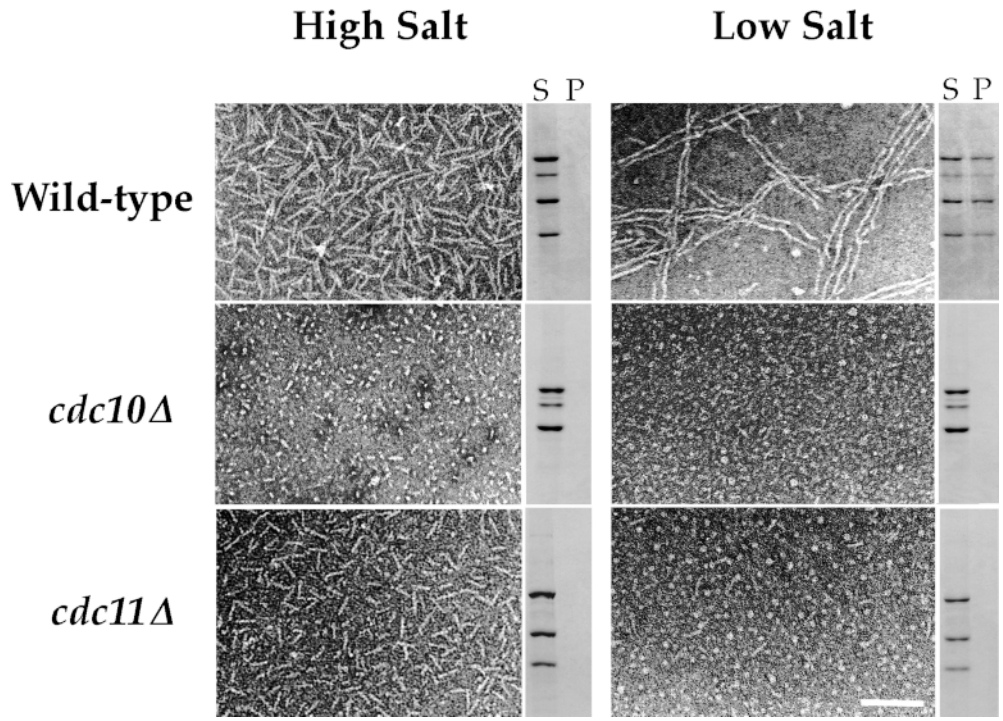

Figure 5. Negative-stain EM and sedimentation assays on wild-type, *cdc10Δ*, and *cdc11Δ* septin complexes in the presence of high- or low-salt buffer. Low-salt samples were prepared by dialyzing septin complexes eluted in the presence of 1 M KCl elution buffer and PVP peptide, at a concentration of 0.07 mg/ml, against 75 mM KCl elution buffer for 30 min at 4°C. After determining the conductivity and protein concentration of the low salt sample, a corresponding high salt sample was prepared by diluting an aliquot of PVP eluate with 1 M KCl elution buffer such that the protein concentration was equal to that of the low-salt sample. An aliquot of each sample was then examined by negative-stain EM, whereas the rest was subjected to centrifugation (90,000 rpm for 20 min) and the resulting supernatant (*S*) and pellet (*P*) samples were analyzed by SDS-PAGE, followed by staining with Coomassie brilliant blue to quantitate the formation of longer sedimentable polymers ($n = 8$). Bar, 100 nm.

structures, the PVP antibody was used to follow Cdc3p localization in wild-type, *cdc10Δ*, and *cdc11Δ* cells. As described previously (Kim et al., 1991), we found that Cdc3p localized to a ring at the mother–bud neck in small-budded and large-budded wild-type cells (Fig. 7, *Wild-type*). In *cdc10Δ* cells, Cdc3p was still found to localize in a ring at the neck in most budded cells (86% versus 97% of wild-type cells; $n = 100$). The ring staining in *cdc10Δ* cells was typically broader and more diffuse than that in wild-type cells, often appearing discontinuous (Fig. 7, *cdc10Δ*). A similar staining pattern has been reported for the Cdc11p antibody in *cdc10Δ* cells (Fares et al., 1996). In most *cdc11Δ* cells, septin staining could not be detected. Weak staining at the neck was observed in ~3% of *cdc11Δ* cells whose morphology was similar to wild type (Fig. 7, *cdc11Δ*), but never in multinucleate cells (Fig. 7, *cdc11Δ*). These results suggest that maintaining septin localization at the neck may be sufficient for septin function in cytokinesis and cell morphogenesis even in the absence of observable neck filaments.

Another process dependent on the septins is the localization of proteins involved in specifying the site of bud emergence (Chant et al., 1995; Sanders and Field, 1995; Longtine et al., 1996; Sanders and Herskowitz, 1996). We examined the localization of one such protein, Bud4p, in wild-type, *cdc10Δ*, and *cdc11Δ* cells to monitor septin function in the absence of observable neck filaments. As described by Sanders and Herskowitz (1996), we found that Bud4p localizes to one or two discrete rings at the mother–bud neck in large-budded wild-type cells (Fig 8, *Wild-type*). In most large-budded *cdc10Δ* cells, Bud4p was still localized to the neck (Fig. 8, *cdc10Δ*). The Bud4p neck staining that was observed, however, was typically broader and more punctate than that observed in wild-type cells, and in many cases only a dot of staining was detected at the neck (Table III). Moreover, the apparent double rings commonly observed in wild-type cells were not observed in the *cdc10Δ* strain. To assess whether the diffusely localized Bud4p in *cdc10Δ* cells was still functional in axial bud-site selection, we examined the pattern of bud scars in wild-type and *cdc10Δ* haploid cells by Calcofluor staining (see Materials and Methods). In 91% of wild-type and 58% of *cdc10Δ* haploid cells bud scars were aligned in a single chain, indicating that axial budding is occurring with some efficiency in the *cdc10Δ* strain. In *cdc11Δ* cells, no Bud4p staining could be detected. Even at high detection sensitivity, only background spindle staining similar to that described in Sanders and Herskowitz (1996) was seen (Fig. 8, *cdc11Δ*) (Table III). Thus, Bud4p localization and efficient axial budding, a marker for one aspect of septin function, was observed in *cdc10Δ* but not *cdc11Δ* cells.

Discussion

Septin Complex Structure and Polymerization

We have purified a protein complex containing the four yeast septins Cdc3p, Cdc10p, Cdc11p, and Cdc12p. When high-salt preparations of this complex are visualized by negative-stain EM, short filaments with lengths that are multiples of 32 nm are observed. This suggests that the yeast septin complex forms a 32-nm filament subunit that

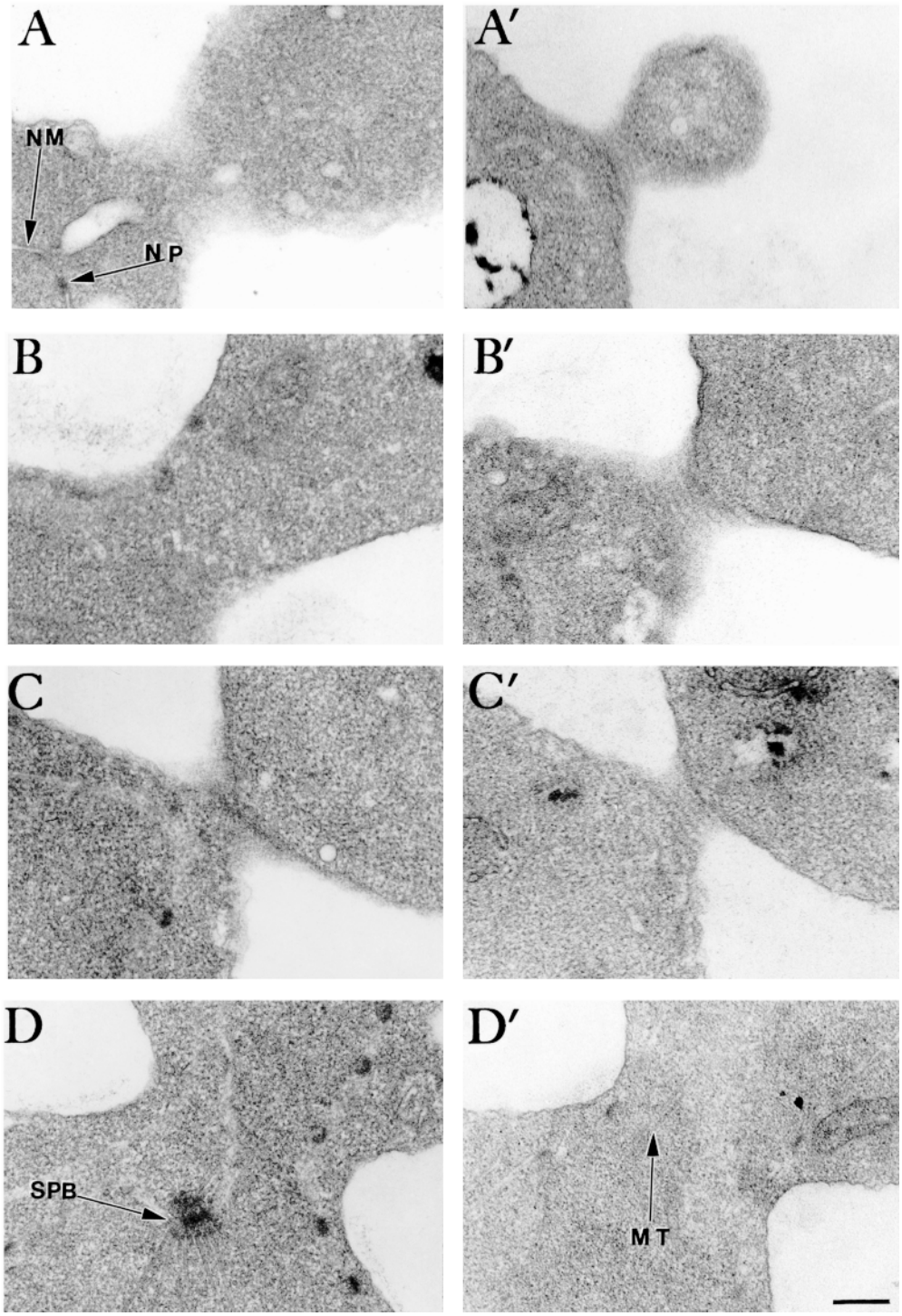

Figure 6. Thin-section EM of neck regions in wild-type, *cdc10Δ*, and *cdc11Δ* cells. (*A* and *B*) Grazing sections of bud necks in *cdc11Δ* cells as observed in two different rounds of embedding and sectioning. (*C*) A grazing section of a typical *cdc10Δ* neck. (*D*) The *cdc10Δ* cell observed to have dots along the inside of the plasma membrane that might be neck filaments in cross section (*arrowhead*). Grazing (*A′–C′*) and cross (*D′*) sections of wild-type cells showing neck filaments as surface striations or as dots (*arrowheads*). *Arrows*, cellular features: *NM*, nuclear membrane; *NP*, nuclear pore; *PM*, plasma membrane; *SPB*, spindle pole body; *MT*, microtubule. Bar, 200 nm.

associates endwise to form linear polymers. These results are consistent with similar studies of septin complexes purified from *Drosophila* and mammalian cells (Field et al., 1996; Hsu et al., 1998), and indicate that in addition to protein sequence and a role in cytokinesis, aspects of septin complex assembly and polymerization have been conserved.

Although the structural similarity between septin complexes from different species is striking, how these complexes are assembled from different numbers of divergent septin polypeptides is unclear. A simple model for the organization of the *Drosophila* septin complex (Field et al., 1996) proposed that septin polypeptides homodimerize and align end on end, with the length of the subunit determined by the additive length of the coiled-coil domains. Our analysis of septin complexes purified from different yeast strains does not support this simple model. First, in the absence of Cdc10p, a protein that is not predicted to contain a coiled-coil domain, the subunit length is significantly shorter. Second, in the absence of Cdc11p, a protein

Table II. Neck Filaments Are Not Observed in cdc10Δ or cdc11Δ Cells

Genotype	No filaments	Filaments*	
		In cross section	In grazing section
Wild-type	67	76	57
cdc10Δ	148	1	0
cdc11Δ	150	0	0

*Following Byers and Goetsch (1976), dots spaced at intervals of ~32 nm on the inside of the plasma membrane in cross sections of the neck region were counted as neck filaments, as were striations with a spacing of ~32 nm observed in grazing sections of the plasma membrane.

with a coiled-coil domain, the length of the septin subunit is often the same as wild-type. In addition, doubling the coiled-coil domain of Cdc3p has no effect on subunit length (Frazier, J.A., unpublished data). Based on these results, we suspect that septin complex structure is not as straightforward as in the model proposed by Field et al. (1996). Reassembly of septin complexes from individual proteins and higher resolution structural studies should provide further insight into the organization and conservation of the septin filament subunit.

Evidence for Septin Polymerization In Vivo

The yeast septins are thought to be the major structural components of a highly ordered structure at the mother–bud neck, the neck filaments (Cooper and Kiehart, 1996; Longtine et al., 1996). In support of this hypothesis, we have shown that septin complexes purified from wild-type cells can form long polymers in vitro. Furthermore, when we purify the septin complexes from *cdc10Δ* or *cdc11Δ* strains, in which neck filaments cannot be detected, in vitro polymerization is severely compromised. Although these results strongly suggest that septin polymerization is required for formation of the neck filaments in vivo, the relationship between the septin filaments and the neck filaments remains unclear. The 10-nm striations that are ob-

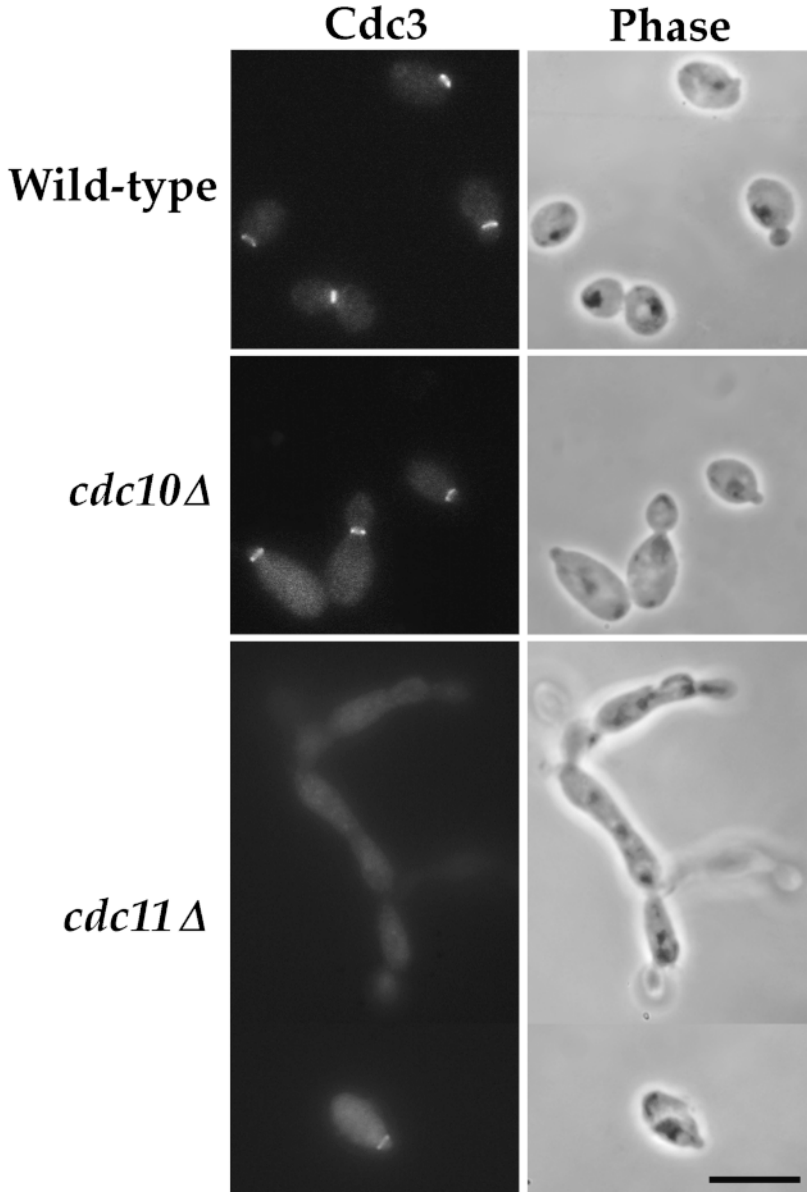

Figure 7. Septin localization by immunofluorescence and the corresponding phase–contrast micrographs of wild-type, *cdc10Δ*, and *cdc11Δ* cells. Note that the two cells shown in the *cdc11Δ* panel are from different fields of the same slide. The multinucleate *cdc11Δ* cells in this figure are representative of strain morphology after treatment with zymolyase. Cells were grown in YPD medium to early log-phase at 22°C. Bar, 10 μm.

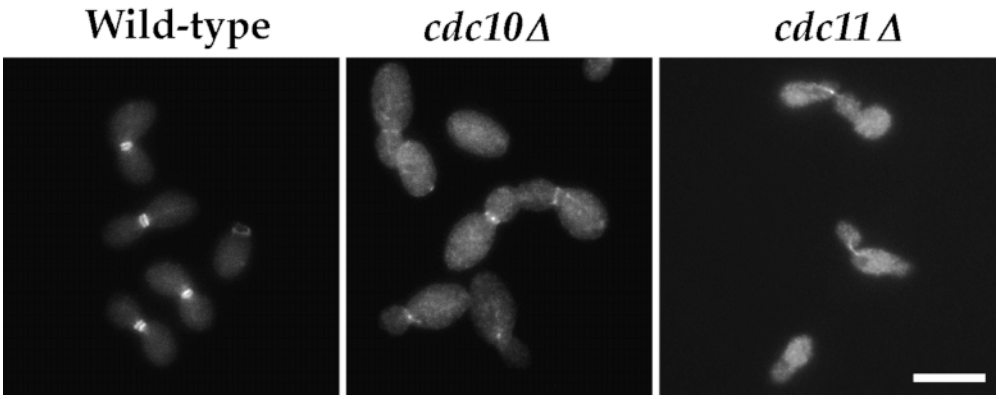

Figure 8. Bud4p localization in wild-type, *cdc10Δ*, and *cdc11Δ* cells. Cells were grown in YPD medium to early log phase at 22°C, fixed, and processed for indirect immunofluorescence using affinity-purified Bud4p antibodies (provided by S. Sanders Massachusetts Institute of Technology, Boston, MA). Images of Bud4p staining in septin deletion strains were taken at higher exposures than the corresponding wild-type images. Bar, 10 μm.

served at the bud neck of wild-type cells by thin-section EM could correspond to the septin polymers themselves or may result from the organization of the septin filaments into a more highly ordered array. Alternatively, the neck filaments may be composed of another protein whose assembly is dependent on septin polymerization or organization. Although we suspect that the absence of neck filaments in *cdc10Δ* and *cdc11Δ* cells is due to a failure in septin polymerization, it is possible that the mutant septin complexes do polymerize in vivo but fail to form an organized structure that is detectable by EM.

The septins purified from wild-type yeast cells were observed to form extensive filament pairs under low salt conditions. Such pairing has not been observed with purified *Drosophila* or mammalian septin complexes (Field et al., 1996; Hsu et al., 1998). It is possible that the pairing observed in our work reflects the presence of a higher order septin filament structure that occurs in yeast and not higher eukaryotic cell types. How the filament pairing is mediated is unclear, as we were unable to detect any structure between the filaments by negative-stain EM. This interaction may be regulated by phosphorylation, a possibility suggested by recent studies of septin organization in the absence of the Gin4p protein kinase (Longtine et al., 1998). In cells deleted for *GIN4*, the septins reorganize from an apparent ring to a set of discrete bars running through the mother–bud neck. Thus Gin4p, which appears unique to yeasts, may be responsible for the assembly of a higher order septin filament structure.

Implications for Septin Function

Studies of conditional septin alleles at the nonpermissive temperature have shown that the septins are required for cytokinesis, normal cell morphology, and the localization of a number of proteins (like Bud4p) to the neck in budding yeast (Hartwell, 1971; Chant et al., 1995; Sanders and Herskowitz, 1996; DeMarini et al., 1997; Lippincott and Li, 1998). The disruption of these processes in conditional septin mutants is correlated with the loss of both septin localization at the neck by immunofluorescence and neck filaments by EM (Haarer and Pringle, 1987; Ford and Pringle, 1991; Kim et al., 1991). These observations, combined with biochemical evidence that septins form filaments, suggest that polymerization is central to septin function. In this study we show that two septin mutant strains, *cdc10Δ* and *cdc11Δ*, appear to be defective for septin polymerization; these cells lack neck filaments and septin complexes purified from these strains fail to polymerize. To assess the role of polymerization in septin function, we monitored septin dependent processes like cytokinesis, cell morphogenesis, and Bud4p localization in these cells.

Table III. Localization of Bud4p in Large-budded Cells

		Localization to neck	
Genotype	No localization	Ring	Other structure*
Wild-type	0	100	0
cdc10Δ	9	76	15
cdc11Δ	96	1	3

*See text.

The *cdc11Δ* strain was similar to previously characterized conditional septin alleles, in that septin-dependent processes were severely compromised. This loss of septin function correlated with a loss of both septin localization by immunofluorescence and detectable neck filaments by EM. The *cdc10Δ* strain, in contrast, was unlike existing septin mutants. Although no neck filaments could be detected by EM in these cells, the septins still localized to the bud neck. The uncoupling of filament formation and protein localization in this strain allows us to draw new conclusions about the role of polymerization in septin function. *cdc10Δ* cells maintained a considerable degree of septin function as assayed by cytokinesis, cell morphology, and the localization of Bud4p. This suggests that the localization of the septins to the neck region is more critical for septin function than the dynamics of septin polymerization or the formation of a neck filament structure. This conclusion is supported by studies of septin organization in cells that do not contain the kinase Gin4p (Longtine et al., 1998). Despite a dramatic reorganization of the septins (from a continuous ring to a set of axial bars running through the mother–bud neck) in these cells, the septins appear to function almost normally.

If the septins function in cytokinesis and other processes in the absence of normal septin polymerization or the assembly of a neck filament structure, it is unclear why the ability of septin complexes to form filaments has been conserved. In this regard it is important to distinguish between polymerization per se and the assembly of the polymers

into higher order filament arrays. The assembly of a higher order filament array may in fact be unique to asymmetrically dividing cells. To date, septin-associated filament arrays have been observed only at the mother–bud necks in *S. cerevisiae* and *C. albicans* (Byers and Goetsch, 1976; Soll and Mitchell, 1983). It is possible that the neck filament array functions in these cell types to constrain the membrane at the division site during growth of the daughter cell. However, the assembly of a neck filament-like structure is unlikely to be the only function of septin polymerization. A septin-associated filament array has never been observed in *Drosophila* or mammalian cells, yet septin complexes purified from these cell types are capable of polymerization. It seems likely that these cells contain septin filaments, but these filaments may be difficult to detect if not organized into a neck filament-like array.

Our data suggests that the polymerization enhances, but is not required for, septin function. For example, local concentration of the septin GTPase domains by polymerization could facilitate the rapid recruitment of proteins involved in polarity and division to the division site. At different points in the cell cycle, the nucleotide-binding state of the septin proteins may serve as a "switchboard," regulating the localization of the bud site selection machinery (Bud3p and Bud4p) (Chant et al., 1995; Sanders and Herskowitz, 1996), proteins involved in bud growth (Gin4p) (Longtine et al., 1998), cytokinesis (MyoIp) (Lippincott and Li, 1998), and chitin deposition (Chs3, Bni4p, and Chs4p) (DeMarini et al., 1997). Although the actual role of the septins in cytokinesis and other processes is not clear, the results presented in this study suggest that this function may not require normal septin polymerization or the formation of a neck filament array. In light of this data, we argue that the septins should not be classified as a novel cytoskeletal filament, as the formation of in vivo filament structures, and the dynamics of the filaments from which these structures are composed, are central to the function of classic cytoskeletal filaments composed of actin, intermediate filament proteins, or tubulin.

We thank members of the Mitchison and Alberts labs, past and present, for providing a stimulating and supportive environment. We are particularly grateful to P. Coughlin (Harvard University, Cambridge, MA), K. McDonald (University of California, Berkeley, CA), J. Heuser (Washington University, St. Louis, MO), I. Adams, and J. Kilmartin (both from Medical Research Council, Cambridge, UK) for valuable discussions on electron microscopy; J. Hartman, N. Pollock, and R. Vale (all three from University of California, San Francisco, CA) for help with DIC microscopy; C. Carroll, D. Kellogg (both from University of California, Santa Cruz, CA), and S. Sanders for yeast strains, antibodies, and helpful discussions; and B. Alberts, A. Desai, M. Lenburg, K. Oegema, J. Rosenblatt, C. Walczak, and M. Welch (all seven from University of California, San Francisco, CA) for technical assistance, encouragement, and critical comments on this manuscript.

This work was supported by National Institutes of Health grants to T.J. Mitchison (GM-23928) and J.R. Pringle (GM-31006). J.A. Frazier is a National Science Foundation predoctoral fellow, and M.L. Wong is supported by the Howard Hughes Medical Institute.

Received for publication 13 August 1998 and in revised form 1 October 1998.

References

Alberts, B., D. Bray, J. Lewis, M. Raff, K. Roberts, and J.D. Watson. 1994. Molecular Biology of the Cell. M. Richardson, editor. Garland Publishing, New York. 1,294 pp.

Amos, L., and W.B. Amos. 1991. Molecules of the Cytoskeleton. *In* Macmillan Molecular Biology Series. C. Skidmore, editor. Macmillan Education Ltd., London, UK. 193 pp.

Baudin, A., O. Ozier-Kalogeropoulos, A. Denouel, F. Lacroute, and C. Cullin. 1993. A simple and efficient method for direct gene deletion in *Saccharomyces cerevisiae*. *Nucleic Acids Res.* 21:5067–5076.

Bi, E., and J.R. Pringle. 1996. *ZDS1* and *ZDS2*, genes whose products may regulate Cdc42p in *Saccharomyces cerevisiae*. *Mol. Cell. Biol.* 16:5264–5275.

Bourne, H.R., D.A. Sanders, and F. McCormick. 1991. The GTPase superfamily: conserved structure and molecular mechanism. *Nature*. 349:117–127.

Byers, B., and L. Goetsch. 1976. A highly ordered ring of membrane-associated filaments in budding yeast. *J. Cell Biol*. 69:717–721.

Byers, B., and L. Goetsch. 1991. Preparation of yeast cells for thin-section electron microscopy. *Methods Enzymol*. 194:602–608.

Carroll, C.W., R. Altman, D. Schieltz, J. Yates, and D. Kellogg. 1998. The septins are required for the mitosis-specific activation of the Gin4 kinase. *J. Cell Biol.* 143:709–717.

Chant, J., M. Mischke, E. Mitchell, I. Herskowitz, and J.R. Pringle. 1995. Role of Bud3p in producing the axial budding pattern of yeast. *J. Cell Biol*. 129: 767–778.

Cooper, J.A., and D.P. Kiehart. 1996. Septins may form a ubiquitous family of cytoskeletal filaments. *J. Cell Biol*. 134:1345–1348.

De Virgilio, C., D.J. DeMarini, and J.R. Pringle. 1996. *SPR28*, a sixth member of the septin gene family in *Saccharomyces cerevisiae* that is expressed specifically in sporulating cells. *Microbiology*. 142:2897–2905.

DeMarini, D.J., A.E.M. Adams, H. Fares, C. De Virgilio, G. Valle, J.S. Chuang, and J.R. Pringle. 1997. A septin-based hierarchy of proteins required for localized deposition of chitin in the *Saccharomyces cerevisiae* cell wall. *J. Cell Biol*. 139:75–93.

Fares, H., L. Goetsch, and J.R. Pringle. 1996. Identification of a developmentally regulated septin and involvement of the septins in spore formation in *S. cerevisiae*. *J. Cell Biol.* 132:399–411.

Fares, H., M. Peifer, and J.R. Pringle. 1995. Localization and possible functions of *Drosophila* septins. *Mol. Biol. Cell*. 12:1843–1859.

Field, C.M., O.S. Al-Awar, J. Rosenblatt, M.L. Wong, and B. Alberts. 1996. A purified *Drosophila* septin complex forms filaments and exhibits GTPase activity. *J. Cell Biol*. 133:605–616.

Flescher, E.G., K. Madden, and M. Snyder. 1993. Components required for cytokinesis are important for bud site selection in yeast. *J. Cell Biol.* 122:373–386.

Ford, S.K., and J.R. Pringle. 1991. Cellular morphogenesis in the *Saccharomyces cerevisiae* cell cycle: localization of the *CDC11* gene product and the timing of events at the budding site. *Dev. Genet.* 12:281–292.

Fuchs, E., and D.W. Cleveland. 1998. A structural scaffolding of intermediate filaments in health and disease. *Science*. 279:514–519.

Gietz, R.D., and A. Sugino. 1988. New yeast-*Escherichia coli* shuttle vectors constructed with in vitro mutagenized yeast genes lacking six-base pair restriction sites. *Gene*. 74:527–534.

Guthrie, C., and G.R. Fink. 1991. Guide to Yeast Genetics and Molecular Biology. *Methods Enzymol*. 194:1–93.

Haarer, B.K., and J.R. Pringle. 1987. Immunofluorescence localization of the *Saccharomyces cerevisiae CDC12* gene product to the vicinity of the 10-nm filaments in the mother-bud neck. *Mol. Cell Biol*. 7:3678–3687.

Hartwell, L.H. 1971. Genetic control of the cell division cycle in yeast. IV. Genes controlling bud emergence and cytokinesis. *Exp. Cell Res.* 69:265–276.

Hsu, S.C., C.D. Hazuka, R. Roth, D.L. Folettie, J. Heuser, and R.H. Scheller. 1998. Subunit composition, protein interactions, and structures of the mammalian brain sec6/8 complex and septin filaments. *Neuron*. 20:1111–1122.

Jones, J., and L. Prakash. 1990. Yeast *Saccharomyces cerevisiae* selectable markers in pUC18 polylinkers. *Yeast*. 6:363–366.

Kato, K. 1990. A collection of cDNA clones with specific expression patterns in the mouse brain. *Eur. J. Neurosci.* 2:704–711.

Kellogg, D.R., T. Kikuchi, T. Fujii-Nakata, C.W. Turck, and A.W. Murray. 1995. Members of the NAP/SET family of proteins interact specifically with B-type cyclins. *J. Cell Biol.* 130:661–673.

Kim, H.B., B.K. Haarer, and J.R. Pringle. 1991. Cellular morphogenesis in the *Saccharomyces cerevisiae* cell cycle: localization of the *CDC3* gene product and the timing of events at the budding site. *J. Cell Biol*. 112:535–544.

Kinoshita, M., S. Kumar, A. Mizoguchi, C. Ide, A. Kinoshita, T. Haraguchi, Y. Hiraoka, and M. Noda. 1997. Nedd5, a mammalian septin, is a novel cytoskeletal component interacting with actin-based structures. *Genes Dev*. 11: 1535–1547.

Kumar, S., Y. Tomooka, and M. Noda. 1992. Identification of a set of genes with developmentally down-regulated expression in the mouse brain. *Biochem. Biophys. Res. Commun*. 185:1155–1161.

Lippincott, J., and R. Li. 1998. Sequential assembly of myosin II, an IQGAP-like protein, and filamentous actin to a ring structure involved in budding yeast cytokinesis. *J. Cell Biol*. 140:355–366.

Longtine, M.S., D.J. DeMarini, M.L. Valencik, O.S. Al-Awar, H. Fares, C. De Virgilio, and J.R. Pringle. 1996. The septins: roles in cytokinesis and other processes. *Curr. Opin. Cell Biol*. 8:106–119.

Longtine, M.S., H. Fares, and J.R. Pringle. 1998. Role of the yeast Gin4p protein kinase in septin assembly and the relationship between septin assembly and septin function. *J. Cell Biol.* 143:719–736.

Mitchell, D.A., T.K. Marshall, and R.J. Deschenes. 1993. Vectors for the induc-

ible overexpression of glutathione S-transferase fusion proteins in yeast. *Yeast*. 9:715–723.

Nakatsura, S., K. Sudo, and Y. Nakamura. 1994. Molecular cloning of a novel human cDNA homologous to *CDC10* in *Saccharomyces cerevisiae*. *Biochem. Biophys. Res. Commun.* 202:82–87.

Neufeld, T.P., and G.M. Rubin. 1994. The *Drosophila peanut* gene is required or cytokinesis and encodes a protein similar to yeast putative bud neck filament proteins. *Cell*. 77:371–379.

Nottenburg, C., W.M. Gallatin, and T. St. John. 1990. Lymphocyte HEV adhesion variants differ in the expression of multiple gene sequences. *Gene*. 95: 279–284.

Novick, P., and D. Botstein. 1985. Phenotypic analysis of temperature-sensitive yeast actin mutants. *Cell*. 40:405–416.

Pringle, J.R., A.E. Adams, D.G. Drubin, and B.K. Haarer. 1991. Immunofluorescence methods for yeast. *Methods Enzymol.* 194:565–602.

Sambrook, J., E.F. Fritsch, and T. Maniatis. 1989. Molecular Cloning: A Laboratory Manual. 2nd ed. Cold Spring Harbor Laboratory Press, Cold Spring Harbor, NY.

Sanders, S.L., and C.M. Field. 1995. Bud-site selection is only skin deep. *Curr. Biol.* 5:1213–1215.

Sanders, S.L., and I. Herskowitz. 1996. The Bud4 protein of yeast, required for axial budding, is localized to the mother–bud neck in a cell cycle-dependent manner. *J. Cell Biol*. 134:413–427.

Sawin, K.E., T.J. Mitchison, and L.G. Wordeman. 1992. Evidence for kinesin-related proteins in the mitotic apparatus using peptide antibodies. *J. Cell Sci*. 101:303–313.

Siegel, L., and K. Monty. 1966. Determination of molecular weights and frictional ratios of proteins in impure systems by use of gel filtration and density gradient centrifugation. Application to crude preparations of sulfite and hydroxylamine reductases. *Biochim. Biophys. Acta*. 112:346–362.

Sikorski, R.S., and P. Hieter. 1989. A system of shuttle vectors and yeast host strains designed for efficient manipulation of DNA in *Saccharomyces cerevisiae*. *Genetics*. 122:19–27.

Soll, D.R., and L.H. Mitchell. 1983. Filamentous ring formation in the dimorphic yeast *Candida albicans*. *J. Cell Biol.* 96:486–493.

Witke, W., A.V. Podtelejnikov, A. Di Nardo, J.D. Sutherland, C. Dotti, and M. Mann. 1998. In mouse brain profilin I and profilin II associate with regulators of the endocytic pathway and actin assembly. *EMBO (Eur. Miol. Biol. Organ.) J.* 17:967–976.

Zheng, Y., M.L. Wong, B. Alberts, and T. Mitchison. 1996. Nucleation of microtubule assembly by a g-tubulin containing ring complex. *Nature*. 378: 578–583.